

# Journal of Astronomical Telescopes, Instruments, and Systems

AstronomicalTelescopes.SPIEDigitalLibrary.org

## **Subaru Portable Spectrophotometer: *in-situ* reflectivity measurement for large telescope mirror**

Hirofumi Okita  
Naruhisa Takato  
Saeko S. Hayashi

**SPIE.**

Hirofumi Okita, Naruhisa Takato, Saeko S. Hayashi, "Subaru Portable Spectrophotometer: *in-situ* reflectivity measurement for large telescope mirror," *J. Astron. Telesc. Instrum. Syst.* **5**(1), 014002 (2019), doi: 10.1117/1.JATIS.5.1.014002.

# Subaru Portable Spectrophotometer: *in-situ* reflectivity measurement for large telescope mirror

Hirofumi Okita,<sup>a,\*</sup> Naruhisa Takato,<sup>a</sup> and Saeko S. Hayashi<sup>a,b</sup>

<sup>a</sup>Subaru Telescope, National Astronomical Observatory of Japan, Hilo, Hawaii, United States

<sup>b</sup>TMT-J Project Office, National Astronomical Observatory of Japan, Tokyo, Japan

**Abstract.** The reflectivity of a telescope primary mirror is one of the fundamental parameters that determines the telescope performance. Due to a lack of suitable instruments, however, measuring the absolute value of the reflectivity, in particular wide spectral measurements *in-situ*, has been almost impossible. To solve this problem, we developed a portable spectrophotometer called the Subaru Portable Spectrophotometer (SPS). SPS covers a spectral range between 380 and 1000 nm with a resolution of 2 nm. Its dimension and weight enable *in-situ* measurement on the primary mirror. A modified V-N method is applied to SPS for obtaining the absolute reflectivity. A sequential measurement makes SPS compensate the instrumental drift. The great advantage of SPS is its capability of getting absolute spectral reflectivity *in-situ*, even after the primary mirror is mounted on a telescope. In the case of Subaru Telescope, SPS clarified the reflectivity of the primary mirror coated with aluminum 4 years ago. Periodic measurements have been on-going since the primary mirror recoating in 2017. It is now possible to study the telescope reflectivity degradation with SPS. © The Authors. Published by SPIE under a Creative Commons Attribution 4.0 Unported License. Distribution or reproduction of this work in whole or in part requires full attribution of the original publication, including its DOI. [DOI: [10.1117/1.JATIS.5.1.014002](https://doi.org/10.1117/1.JATIS.5.1.014002)]

Keywords: reflectivity; *in-situ* measurement; spectrophotometer; telescope primary mirror; Subaru Telescope.

Paper 18065 received Aug. 14, 2018; accepted for publication Dec. 26, 2018; published online Jan. 22, 2019.

## 1 Introduction

Reflectivity degradation is one of the biggest problems for astronomical telescopes. Since the reflectivity degradation directly affects the efficiency of observations night by night, a longer and longer integration time is required to obtain data with the same quality at the time of the mirror coating. To recover its reflectivity, recoating works are carried out periodically for large telescope's mirrors at many observatories. However, the recoating work requires weeks to months downtime, which reduces observing opportunities, and increases the risk of damaging the mirrors.

There are two main mechanisms that cause the reflectivity degradation: chemical reactions and physical effects. The chemical reactions include oxidization and corrosion on a mirror surface. An oxide formation of less than 2 nm thickness on a fresh aluminum (Al) coating affects the reflectivity at far ultraviolet.<sup>1</sup> In contrast, a few nanometer thickness oxide formation rarely contribute to the reflectivity degradation at visible wavelength. Surface corrosion occurs when dust particles on the mirror surface absorb moisture from ambient environment. There is natural Al<sub>2</sub>O<sub>3</sub> coating formed on the Al mirror surface rapidly in the atmosphere, and this becomes a good protector. However, it does not sufficiently protect Al from moisture.<sup>2</sup> Dust on the surface and humidity around the environment creates acids or alkalis, and then corrosion on the surface occurs. Glycol, which is broadly used as a coolant, is also extremely corrosive and can eventually degrade to form acids that increases the acidity and further accelerate corrosion when it leaks on the mirror surface.<sup>3</sup>

The physical effects include accumulation of dust and micro-scratches by dust on the mirror surface. Dust accumulates on

a mirror surface and, as a result, the reflectivity becomes low. The surface dust also becomes the cause of scattering and they also reduce the reflectivity. Fortunately, the surface dust can be removed by washing and there is no reflectivity reduction observed at 670 nm.<sup>4</sup> However, the nonrecoverable roughness of the surface is attributed to the numerous impacts by dust particles in motion during strong wind periods and it reduces the reflectivity.<sup>5</sup> The micro scratches on the surface are not recoverable by any cleanings, and it requires recoating.

Many observatories have been monitoring the reflectivity of their primary mirrors at specific wavelength(s). For example, the reflectivity degradation at the Canada–France–Hawaii Telescope (CFHT) on Maunakea was 2.87% per year at 670 nm unless the mirror was CO<sub>2</sub> cleaned.<sup>4</sup> The reflectivity degradation at the Gran Telescopio Canarias in La Palma, the Canary Islands was reported about 7.3% per year.<sup>6</sup> The reflectivity degradation at Subaru Telescope was also reported.<sup>7</sup> These studies used single or a few wavelengths data due to a lack of suitable measuring instruments.

Many efforts have been made to prevent the reflectivity degradation. *In-situ* CO<sub>2</sub> cleaning is a typical technique. For example, the reflectivity degradation at CFHT became 1.96% per year using this technique.<sup>4</sup> However, for a dirty mirror, especially the one whose reflectivity is below 85% to 86% at 670 nm, it is difficult to remove dust from the mirror.<sup>6,8</sup> CO<sub>2</sub> cleaning is less effective and rather produces stripes on the mirror, which increases the scatter of the measurements.<sup>6</sup> The cost of CO<sub>2</sub> cleaning is another factor of consideration. In the case of Subaru Telescope, CO<sub>2</sub> cleaning requires five size-200 cylinders at a time,<sup>9</sup> which costs about 2500 US dollars per cleaning run (as of 2018).

The reflectivity measurement itself is also a challenging subject for astronomical telescopes. In the previous studies,<sup>3–6,8,10,11</sup> measurements were made mainly by commercially available

\*Address all correspondence to Hirofumi Okita, E-mail: [okita14@naoj.org](mailto:okita14@naoj.org)

portable measuring instruments. Since these portable instruments are calibrated with a reference with known reflectivity, the reflectivity obtained from these instruments is relative. It is impossible to obtain the absolute reflectivity from these. Further, some of these portable instruments use LED(s) or laser(s) as the light source, hence, the reflectivity value is available only at specific wavelength(s). In contrast, a spectrophotometer, which is installed in a laboratory and not for transportation, can give an absolute spectral reflectivity using V-N method and double-beam measurement (see Sec. 2 for detail). However, large optical object like a telescope's primary mirror cannot be measured since such mirror cannot fit the spectrophotometer. A witness sample can give some information about the large optical object, but it is difficult to make the same environment between the witness sample and the large optical object because the two have different dew points due to different thermal capacities. Thus, a witness sample is not suitable for evaluating the aging effect, such as the reflectivity degradation. With these reasons, it has been difficult to obtain the absolute value, especially the wide range spectral reflectivity of an aged telescope's primary mirror.

In this study, we have developed a portable spectrophotometer that is capable of measuring the absolute spectral reflectivity of a telescope's primary mirror *in-situ*. We named the instrument Subaru Portable Spectrophotometer (SPS). Using SPS, we can now monitor the actual reflectivity of a large telescope's primary mirror, even after the primary mirror is mounted on the telescope.

In this paper, we explain the measurement principles in Sec. 2. The instrument design is described in Sec. 3. In Sec. 4, we evaluate the performance. Finally, we show the measurement results at Subaru Telescope in Sec. 5.

## 2 Absolute Measurement Principles

### 2.1 L-V Method

Commercially available spectrophotometers generally use "V-N" method to obtain the absolute reflectivity of an object. V and N refer to the shape of the optical path. Figure 1 shows the optical paths of V-N method.

The light from source A hits three mirrors, M1, M2, and M3, and detector B measures its intensity at the end. The first set of measurement takes the V path, and its luminosity is recorded. By moving M2 location, flipping M3, and placing the sample you want to test at the location shown in Fig. 1, the optical path

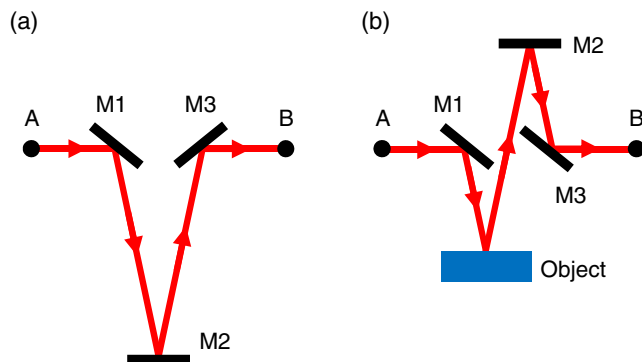


**Fig. 1** Schematic layout of the optical paths of V-N method. (a) Left panel shows the optical path V and (b) right panel shows N.

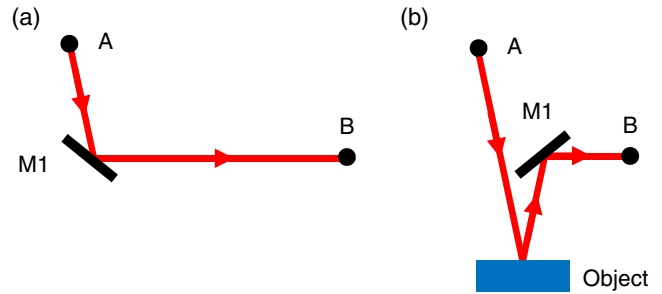


**Fig. 2** Schematic layout of the optical paths of L-V method, which is a modified V-N method. (a) Left panel shows the optical path L and (b) right panel shows V.

becomes N. Then, we measure the luminosity again with the optical path N. Both incident angles of M1, M2, and M3 and the length of the path do not change between V and N. When the luminosity from A is stable and constant, and M2 and M3 have uniform reflectivity, the absolute reflectivity  $R$  of the target object is expressed using the luminosities measured with V path ( $L_V$ ) and N path ( $L_N$ ) as follows:

$$R = L_N/L_V. \quad (1)$$

Our SPS is based on a modified V-N method. From the shape of its optical paths, we named this modified method "L-V" method. Figure 2 shows the optical paths of L-V method. The optical path L works like the optical path V in V-N method, and the path V works like N in V-N. Because the incident angles and optical path lengths are also unchanged in L-V method, the absolute reflectivity  $R$  of the measurement object can again be written with the luminosity  $L_L$  in the optical path L and  $L_V$  in V as follows:

$$R = L_V/L_L. \quad (2)$$

In addition to  $L_L$  and  $L_V$ , measurement at zero incident is necessary as well to subtract background, bias, dark, and readout noise.

### 2.2 Sequence Measurement

Commercial spectrophotometers generally correct the instability (usually called "drift") of a light source and a detector by dividing the light beam into two and getting a reference data continuously and simultaneously. This correction method is generally called double-beams measurement. We did not implement the double-beams mechanism on SPS in order to avoid the weight increase. Instead, we employed a method to correct a drift with sequential measurements. We named this "sequence measurement." Even though the measured luminosity  $L$  fluctuates with time, a short time fluctuation can be approximated by a linear function:

$$L(t) = at + b,$$

where  $a$  and  $b$  are arbitrary constants, and  $t$  is time. Here, we measure luminosities at time  $t - \delta t$ ,  $t$ , and  $t + \delta t$  sequentially:

$$L(t - \delta t) = a(t - \delta t) + b, \quad (3)$$

$$L(t) = at + b, \quad (4)$$

$$L(t + \delta t) = a(t - \delta t) + b. \quad (5)$$

Therefore, we can calculate the luminosity at  $t$  from an average of the luminosity at  $t - \delta t$  and  $t + \delta t$ :

$$\begin{aligned} \{L(t - \delta t) + L(t + \delta t)\} / 2 &= \{a(t - \delta t) + b + a(t + \delta t) + b\} / 2 \\ &= at + b \\ &= L(t). \end{aligned} \quad (6)$$

We can obtain both luminosities of  $L_V$  and  $L_L$  at the same time  $t$  when we measure these in sequence within a short time: the optical path L at  $t - \delta t$ , the optical path V at  $t$ , and the optical path L again at  $t + \delta t$ . Thus, we can compensate the drift and estimate the reflectivity accurately.

### 3 Instrument Design

We have designed SPS with a concept that users can verify whether the measured value is correct by doing optical alignment, L-V calibration, and sequence measurement with the users' responsibility, right before its measurement. Due to this concept, we can manage everything in the SPS's measurement with our own responsibility.

#### 3.1 Light Source

We use a compact and light weighted SLS201L/M Halogen light source manufactured by Thorlabs, Inc., which is equipped with an internal feedback system to achieve a highly stable power output. It has a bulb electrical power of 9 W and color temperature of 2796 K. To obtain collimated beam, two convex lenses ( $f_l = 79$  mm) and a pinhole mask of 1 mm in diameter are mounted in front of the light source. A diaphragm and a cardboard shroud are installed for reducing stray light.

#### 3.2 Detecting Unit

A fiber spectrometer LR1 Configuration B manufactured by ASEQ Instruments is used as the detecting unit of SPS. The detector of LR1 is a Toshiba TCD1304DG linear CCD array, which is broadly used for barcode readings. The spectrometer is calibrated at a particular wavelength by the manufacturer, and we confirmed its calibration using an Argon calibration lamp at Subaru Telescope (Sec. 7.1). The wavelength resolution of a spectrometer depends on the width of the slit and the internal optics of the spectrometer in general. The manufacturer designs the spectrometer with the resolution of 2 nm. Since the pixel scale of the detector is smaller than the resolution, we have developed a software that bins pixels to match the 2 nm resolution.

LR1 spectrometer uses a diffraction grating as a dispersive element, and lights from different orders can overlap. In the case of SPS, no significant detection can be obtained below 350 nm, which means that there are no other orders contamination between 350 and 700 nm. A long-wavelength-path filter which transmits longer than 520 nm covers only a half of the detector. This means that there is also no other orders contamination up to 1040 nm. Therefore, there is no contamination between 350 and 1040 nm on SPS. We did not consider any internal stray lights. An actual measurable wavelength is restricted by the detector sensitivity. We define it as the wavelength range less than 0.6% rms statistical error. From the

statistical evaluation described in Sec. 7.4, the measurable wavelength range of SPS is between 380 and 1000 nm.

An integrating sphere 819D-SL-2 manufactured by Newport Corporation is installed in front of the spectrometer to reduce the incident angle dependence. The integrating sphere strongly attenuates the light beam; however, it preserves the power and is suited for optical power measurement because of the little dependence of the incident angle. The integrating sphere is made with a 2 in. diameter Spectralon, which has over 99% diffuse reflectivity. This small and high reflectivity brings brighter output. A hood for the integrating sphere, which entrance aperture is  $\phi 13$  mm, is attached to reduce stray light.

#### 3.3 Breadboard

The breadboard and the machined parts of SPS have been designed, manufactured, and assembled at the Subaru Telescope machine shop. Figures 3 and 4 show the pictures of SPS in the L and V configurations on the breadboard, respectively.

A flip mirror and a linear guide are installed to keep the incident angles and the length of the optical paths the same between the L and V configurations. Switching the optical paths is operated manually. To change the direction of the light beam from the light source and align the path, a mirror is mounted just behind the collimating optics. Two target plates are used for an alignment purpose.

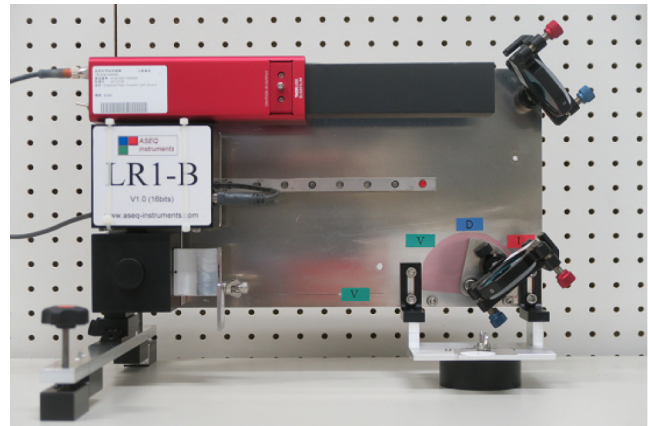


Fig. 3 A photo of SPS at L configuration.

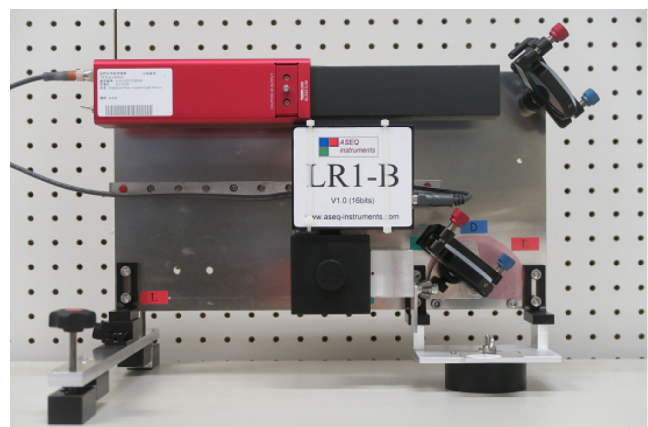


Fig. 4 A photo of SPS at V configuration.

To measure the reflectivity of a large object like a large telescope's primary mirror, SPS should be placed directly on the surface of the target object. For this purpose, we have tried to make SPS as small as possible and as light as possible. The dimension of SPS is 450 mm × 310 mm × 370 mm, and the weight is 5.9 kg. These values mean that SPS is not a hand-held instrument, but it is still transportable and enough compact comparing with a spectrophotometer, which is installed in a laboratory. During the measurement, the device needs to sit on the object directly, and hence, there is a potential that the surface of the object becomes dirty, or the worst case, damaged. To minimize such chances, we have adopted polyoxymethylene plastic (Delrin) legs at the contact points. Nevertheless, after measurement, marks of SPS legs are left on the mirror surface slightly, and thus, the number of measurements should be kept in minimum.

The incident angle on a target object is designed to be 12 deg with a divergent angle of  $\pm 1.6$  deg. For SPS, the light beam from the light source is not completely collimated. Since the Halogen light source is not coherent, the light beam diverges. In order to send the light beam from the light source to the integrating sphere completely, we set the light beam to focus on the entrance of the integrating sphere. The focused image at the entrance of the integrating sphere is the conjugate image of the 1 mm pinhole in the collimating optics, and its diameter at the entrance is  $\sim 6$  mm.

Since the light beam is focused on the entrance of the integrating sphere, the areas of the beam at the flip mirror are different between the L and V configurations. We assume that the reflectivity of the flip mirror is uniform, provided by the fact that the flip mirror is cleaned just before taking the measurement. Because the light beam is not focused on the target surface, but actually it spreads, the diameter of the beam on the measuring surface is relatively large at  $\sim 12$  mm. This large area compensates the local nonuniformity and delivers us a more typical reflectivity of the target object.

The measured value obtained from SPS includes the forward-scattering of the target object. The strength of the forward-scattering depends on the field of measurement, which depends on the entrance aperture of the integrating sphere that corresponds to the size of the pinhole (field stop) of the light source. In the case of SPS, the diameter of the entrance aperture of the integrating sphere is 13 mm, and it corresponds about 5.1 deg in the field of measurement or about 0.006 sr. Thus, the measured value of SPS is the sum of the specular reflectivity and the forward-scattering within 0.006 sr angle. SPS is not able to subtract or correct this effect due to the lack of scattering measurements. To improve the measurement, we will add a scattering measurement function to SPS in the future.

The technical specification of SPS is shown in Table 1. Some parameters of SPS are defined based on the performance evaluations described in Secs. 4 and 7. The list of parts and the drawings of SPS can be downloaded from Ref. 12.

**Table 1** Technical specification of SPS.

Light source	Halogen bulb, 2796 K
Detecting unit	Fiber spectrometer with integrating sphere
Integrating sphere	2-in., Spectralon
Absolute calibration	L-V method
Drift collection	Sequence measurement
Dimensions	450 mm × 310 mm × 370 mm
Weight	5.9 kg
Contact part material	Delrin
Angle of incidence	12 deg $\pm 1.6$ deg
Beam diameter	12 mm
Focus position	Entrance of integrating sphere
Field of measurement	$\phi 5.1$ deg = 0.006 sr
Wavelength range	380 nm to 1000 nm
Wavelength resolution	2 nm
Wavelength accuracy	1 nm rms
Measurement time	5 min
Statistical error	<0.6%rms
Systematic error	<0.2% (alignment and machining errors) $\sim 0.5%$ (unknown)

### 3.4 Software

The spectrometer is controlled by a Windows software distributed by the manufacturer. An in-house software is developed by the author, which bins detector pixels to achieve 2 nm resolution and calculates the reflectivity from the sequence measurement (described in Sec. 2.2). It takes about 5 min to obtain one spectrum dataset.

## 4 Performance Evaluations

In this section, we report the performance of the L-V method and sequence measurement. Comparison measurements with SPS and other measuring instruments are also described. The performance evaluation of the spectrometer itself is shown in Sec. 7.

### 4.1 Systematic Error of L-V Method

In principle, the incident angles and the optical path lengths are unchanged in L-V method; however, due to alignment and machining accuracy, systematic error may occur.

The incident angle dependence of SPS was measured using the light source and the spectrometer after waiting long enough for warming-up. We slightly changed the incident angle to the integrating sphere and measured the relative luminosity. We measured the luminosity at the incident angle of 2 deg and 4 deg and compared them with the one at 0 deg. We measured the luminosity at each incident angle three times each using the sequence measurement. Figure 5(a) shows spectra at 2 deg (blue) and 4 deg (red) incident angles that are divided by 0 deg spectrum. If the incident angle dependence is negligible, the relative luminosity is expected to be 100%, however, the relative luminosity shows offsets of  $\sim 0.18\%$  for 2 deg and

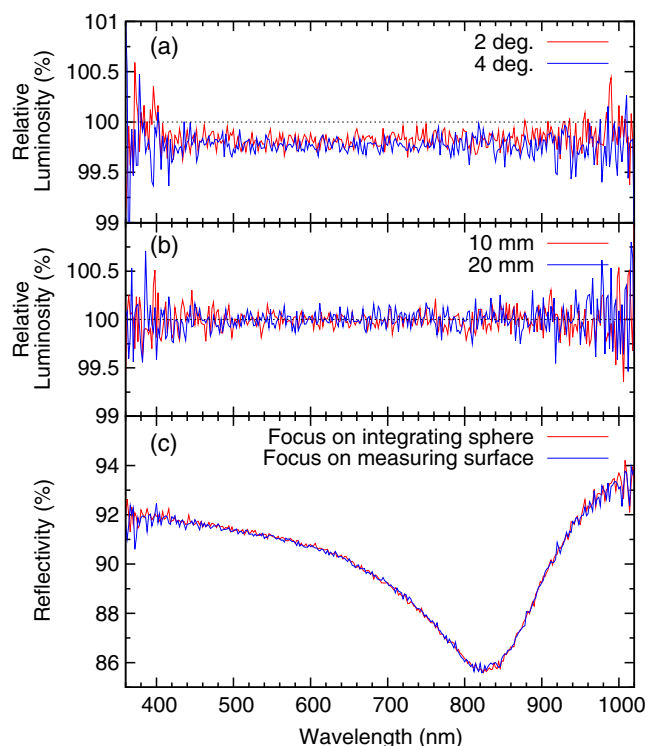


**Fig. 5** Performance evaluations of L-V method. (a) Relative luminosity with different incident angles, (b) relative luminosity with different optical path lengths, and (c) reflectivity comparison with different focus positions.

$\sim 0.23\%$  of 4 deg. There is no wavelength dependence shown in these offsets.

The optical path length dependence of SPS was also evaluated using the light source and the spectrometer which had enough warm-up time, and the result is shown in Fig. 5(b).

To verify the sensitivity, we conducted the following measurement by slightly changing the length of the optical path between the light source and the integrating sphere. We measured the luminosity at a relative optical path length of +10 mm and +20 mm and divided by 0-relative path length measurement to get relative luminosities. At each optical path, three measurements were taken using the sequence measurement. From the evaluation, both relative luminosities (+10 mm and +20 mm) showed neither significant error nor offset. Here, both the incident angle and optical path length errors are from alignment and machining accuracy. Typically, the incident angle error of 1 deg and the optical path length error of a few mm are expected from the alignment and its machining accuracy. Therefore, SPS has less than 0.2% achromatic uncertainty from alignment and machining errors.

We also evaluated the focus position dependence of SPS. As described in Sec. 3.3, SPS sets the light beam to focus on the entrance of the integrating sphere. We measured the reflectivity of a witness sample mirror with this setting three times. Then, we changed the focus position to the target surface and measured the same sample three times. At this setting, one convex lens had to be installed in front of the integrating sphere because the light beam diverged too much to enter the integrating sphere. From the comparison, shown in Fig. 5(c), there was no significant difference in the reflectivity between these two measurements.

## 4.2 Stability of Sequence Measurement

We evaluated the stability of the sequence measurement. First, we evaluated the stability of the light source (drift of the light source) using the light source, which was just turned on, and the spectrometer, which was previously warmed-up enough. We measured the luminosity at the optical path L many times. Figure 6(a) shows the result of the light source instability. The light source is fluctuating about  $\pm 1\%$  relatively even after 30 min.

Second, the stability of the spectrometer (drift of the spectrometer) was measured using the spectrometer, which was just turned on, and the light source, which was previously warmed-up enough. We measured luminosity at the optical path L many times. The result is shown in Fig. 6(b). The spectrometer has  $\sim 1\%$  instability even after 30 min. Here, we note that we were not able to completely separate the instability between the light source and the spectrometer. These two results might be affected by both instability.

Finally, we evaluated the stability of the sequence measurement. We measured the reflectivity of L configuration (instead of V-path) using the sequence measurement. The measured reflectivity was expected to be 100%. The light source and the spectrometer were used right after powering up. We measured the reflectivity every 5 min. Figure 6(c) is the result of the measurements.

The reflectivity of the sequence measurement is a good agreement with the expected value. There was no significant systematic error even immediately after the power-on of the light source and the spectrometer. This means that SPS does

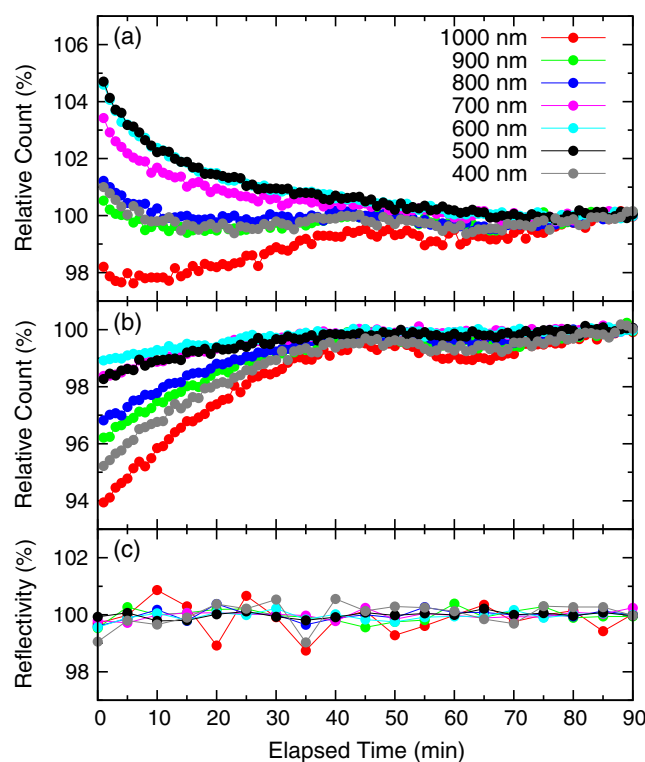


**Fig. 6** Performance evaluations of the sequence measurement. (a) Relative counts at the optical path L with just turn on the light source and enough warm-upped spectrometer, (b) relative counts at the optical path L with just turn on the spectrometer and enough warm-upped light source, and (c) stability of the measured reflectivity with the sequence measurement.

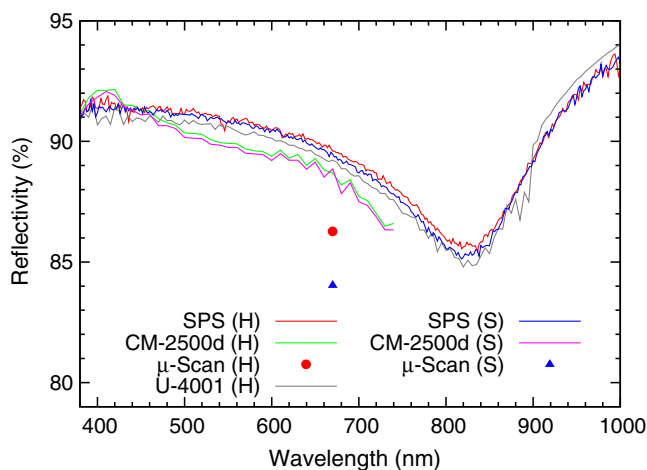


**Fig. 7** Reflectivity of a witness sample mirror obtained from various measuring instruments at Hilo base facility (H) and at the summit facility on Maunakea (S).

not require any warming up time. The short and long end of spectrum has large error [see the lines of 400 nm (gray) and 1000 nm (red) in Fig. 6(c)]. This might be from insufficient sensitivity of the sensor at these wavelengths. The statistical error is described in Sec. 7.4.

#### 4.3 Comparison with Other Measuring Instruments

We compared the reflectivity of a witness sample mirror with other measuring instruments that are available at Subaru Telescope. Hitachi U-4001 is a spectrophotometer at a laboratory in Hilo base facility (~100 m above sea level). The reflectivity obtained from SPS showed ~0.5% offset in visible with respect to the reflectivity from the U-4001 (Fig. 7, gray line). This offset is slightly larger than the expected systematic errors:  $\pm 0.2\%$  in SPS and  $\pm 0.3\%$  in U-4001. Thus, we have to note that SPS has unknown error of ~0.5% in the visible. The cause of this error most likely be from a stray light inside the spectrometer. It may improve when a different spectrometer is used. In any case, these values did not completely correspond, though these were very close.

The reflectivity of the witness sample mirror measured using SPS at sea level and at the summit facility on Maunakea (~4200 m above sea level) was compared and found that they were in good agreement within the statistical and systematic errors (red and blue lines on Fig. 7). We also compared the reflectivity obtained from portable measuring instruments at Hilo and at the summit:  $\mu$ -Scan (Schmitt Measurement Systems, Inc., red circle and blue triangle on Fig. 7) and CM-2500d (Konica-Minolta, Inc., green and purple lines on Fig. 7). Their results were not consistent with the reflectivity from U-4001 nor SPS. The cause of this discrepancy might be from insufficient calibration of  $\mu$ -Scan and CM-2500d.

## 5 Reflectivity Measurements at Subaru Telescope

### 5.1 Reflectivity Before Recoating

The Subaru Telescope primary mirror was recoated with aluminum on October 20, 2017. This was the eighth coating work from its arrival at Maunakea, Hawaii, in 1998 and has been

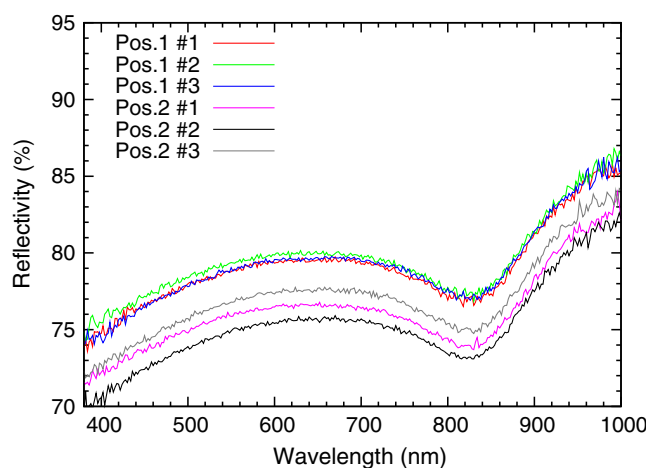


**Fig. 8** Subaru Telescope primary mirror reflectivity before recoating, measured on October 10, 2017.

about 4 years since the previous recoating. Right before the recoating work, the reflectivity was measured with SPS on October 10, 2017.

We measured the reflectivity three times each at two different positions 1 and 2 at the edge of the mirror (See Sec. 8 for positions on the primary mirror used to measure the reflectivity). Figure 8 shows the result. The reflectivity was 70% to 76% at 400 nm, 75% to 80% at 600 nm, and 73% to 78% at 800 nm. We consider that the large dispersion of the reflectivity is from inhomogeneous contamination of the surface, especially from the accumulation of dust particles on the mirror.

Here, we mention that only a few positions on the primary mirror are able to be measured for the Subaru Telescope. There are telescope structures around the primary mirror and those structures restrict accessing to the primary mirror. Thus, we have monitored the reflectivity only at these positions mentioned in Sec. 8.

### 5.2 Reflectivity After Recoating

After the fresh aluminum coating deposited on October 23, 2017, we measured the reflectivity of the primary mirror as soon as it came out of the vacuum chamber. We measured the reflectivity three times at position 1 and two times each at positions 2 and 3. As shown in Fig. 9, the values are 92.1%, 90.5%, and 85.8% at 400 nm, 600 nm, and 800 nm, respectively, with all standard deviation less than 0.6%. Note that the measurements were carried out at the outside of the vacuum chamber, not on the telescope (not *in-situ* measurement). No significant reflectivity dispersion seen before the recoating was observed. After these measurements, the primary mirror was stored inside the vacuum chamber while other telescope works were carried out.

### 5.3 Reflectivity Degradation

We opened again the vacuum chamber to mount the primary mirror to the telescope on November 21, 2017. After that, we continued to monitor the reflectivity *in-situ* on the primary mirror. We measured the reflectivity on January 29, March 7, and April 18, 2018. These days meant 69 days, 106 days, and 148 days, respectively, after the primary mirror started to be exposed to the ambient atmosphere. Each measurement

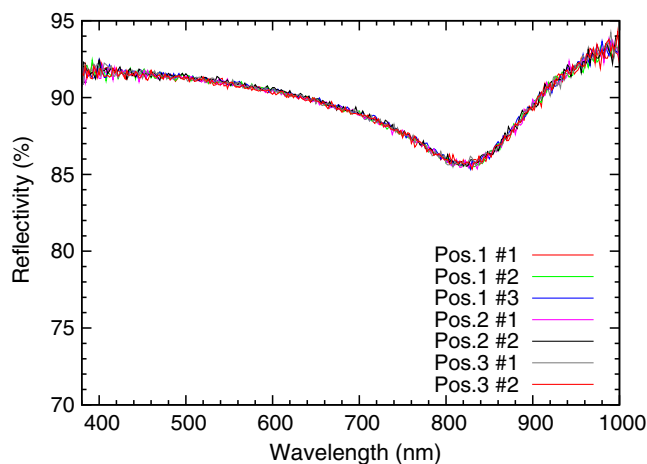


**Fig. 9** Subaru Telescope primary mirror reflectivity right after recoating, measured on October 23, 2017.

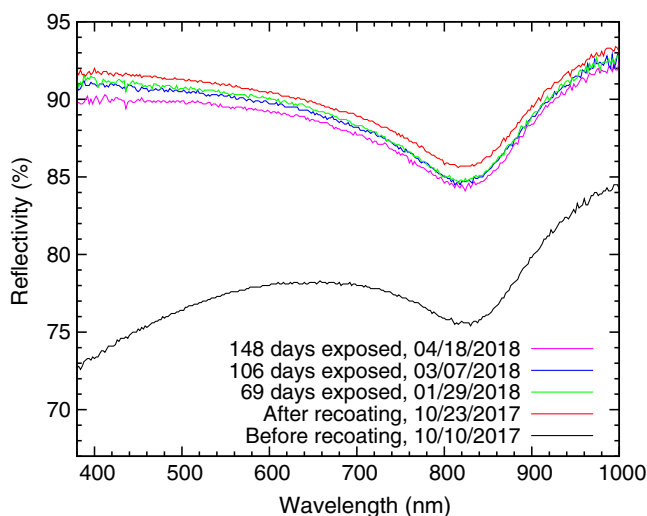


**Fig. 10** Reflectivity of the Subaru Telescope primary mirror before and after the recoating in 2017.

was taken three times at the position 3. We averaged the three measurements, and the results are shown in Fig. 10. The reflectivity of the primary mirror gradually degraded with elapsed time. The reflectivity at shorter wavelength decreases a little faster than that at the longer wavelength. This result means that not only shielding due to dust accumulation but also scattering due to the increase of surface roughness. Since there was a lack of suitable measuring instruments so far, it had been difficult to obtain the absolute spectral reflectivity *in-situ* on a telescope's primary mirror. SPS made it possible. SPS helps us better understanding of the long-term reflectivity degradation.

## 6 Summary

We have developed a portable spectrophotometer named SPS to measure the absolute spectral reflectivity of a telescope's primary mirror *in-situ*. SPS is designed based on a modified V-N method, named "L-V" method (Sec. 2.1), and the sequence measurement (Sec. 2.2) to obtain the absolute reflectivity. SPS covers the spectral range between 380 and 1000 nm with a resolution of 2 nm. Its dimension and weight enable *in-situ*

measurement on the primary mirror even after the primary mirror is mounted on a telescope. In the case of Subaru Telescope, SPS clarified the reflectivity before and after recoating in 2017 and is continuously monitoring the reflectivity. Now it is possible to study the telescope reflectivity degradation with SPS.

## 7 Appendix A: Performance Evaluations of the Spectrometer

### 7.1 Wavelength Accuracy

A wavelength calibration of the spectrometer was performed with a Newport #6030 Argon (Ar) spectral calibration lamp. The calibration lamp was mounted just in front of the integrating sphere of SPS, and data were taken with 300 and 3000 ms exposure, 10 times each. Figure 11 shows the result. By comparing the measured and expected values, some Ar emission lines were identified and used for calibration. Using the Ar lines, the wavelength error of the spectrometer was found to be  $\sim 1$  nm in rms.

### 7.2 Linearity of Dark Frame

Linearity of the dark frame was evaluated with the spectrometer, which was previously warmed-up enough. We put a black cardboard in front of the integrating sphere to make dark environment. We measured dark data at 250 ms, 500 ms, ... up to 3000 ms exposures, 10 times each. Figure 12(a) is the result. Linearity of the dark frame was less than  $\pm 0.4\%$  when the exposure time is less than 1500 ms. If the exposure time is more than 1500 ms, the count did not proportionally increase with time. From this result, the exposure time of SPS measurement is required to be less than 1500 ms.

### 7.3 Linearity of Light Frame

Linearity of the light frame (frames with the light source on) was evaluated using both the light source and the spectrometer, which had enough warm-up time. We assumed that the luminosity was constant and measured it at the optical path L with exposure times of 250 ms, 500 ms, ... up to 3000 ms, 10 times each. Figure 12(b) shows the result. Linearity of the light frame was less than  $\pm 0.4\%$  when the exposure time is less than 1500 ms.

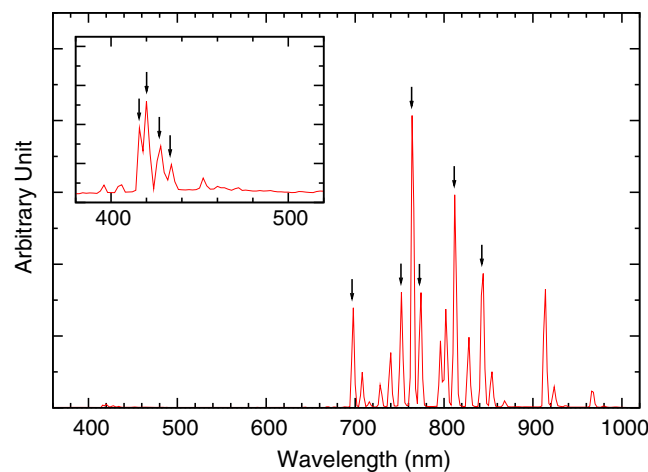


**Fig. 11** Spectrum of an Argon lamp measured by SPS for wavelength calibration purpose. On the top left, a zoomed-in spectrum between 380 and 520 nm is shown for additional lines used in the calibration.

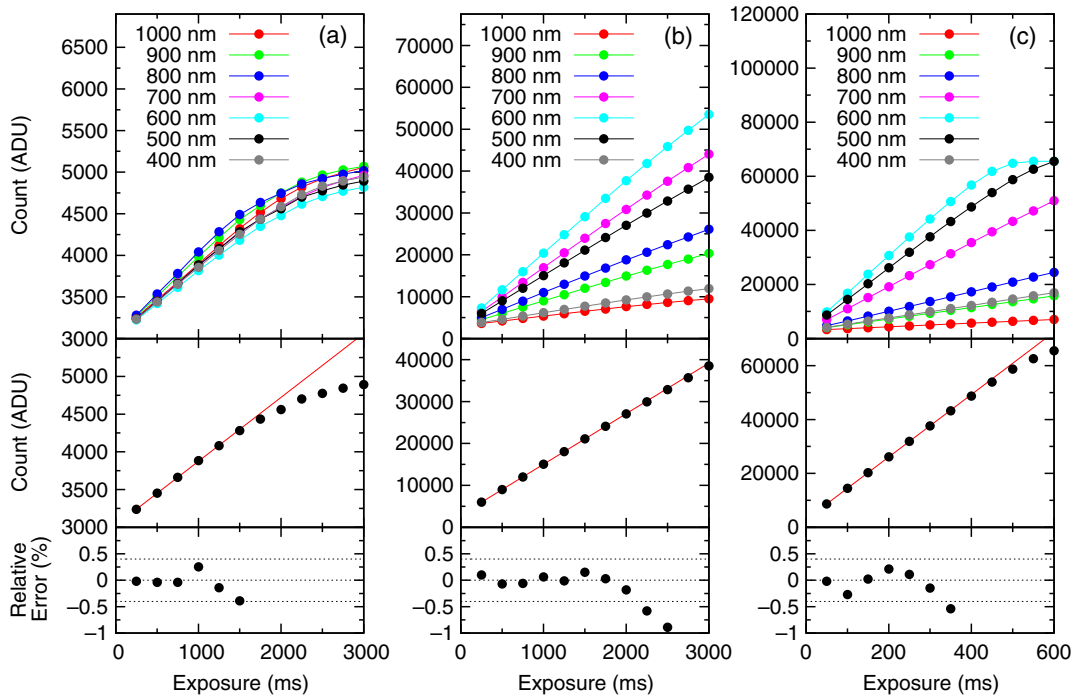


**Fig. 12** (a) Dark frame linearity, (b) light frame linearity with long exposure, and (c) light frame linearity with short exposure. Top panels show the counts with time at various wavelength. Middle panels show the linear fittings at 500 nm. Bottom panels are the relative (residual) errors at 500 nm.

In the case of the exposure time greater than 1500 ms, the count did not proportionally increase with time.

Next, to obtain more count in a shorter exposure time, the integrating sphere was removed from the spectrometer, and an additional evaluation was performed. Figure 12(c) shows the result. Linearity of the light frame was less than  $\pm 0.6\%$  when the count is less than 40,000 ADU. In the case of long exposure time, the count was saturated. From these two evaluations for the light frame, SPS measurement requires the exposure time less than 1500 ms and the count value less than 40,000 ADU. The cause of the nonlinearity at longer exposure time is not sure, though, it might be from the detector and its readout

circuit. The original purpose of the detector is barcode readings and long exposure time is not in consideration.

#### 7.4 Statistical Error

The statistical error of SPS was evaluated using the light source and the spectrometer, both of which were previously warmed-up enough. We measured the reflectivity of the optical path L with the sequence measurement. The measured reflectivity was expected to be 100%. We measured it 18 times and calculated the average and the standard deviation. Figure 13 shows the result. From the standard deviation of the reflectivity, the statistical error was less than 0.2% in rms at the wavelength between 450 and 900 nm. The statistical error at 380 to 450 nm and 900 to 1000 nm was also less than  $\sim 0.6\%$  in rms. Due to relatively small amount of luminosity at short and long wavelengths, the standard deviation is relatively large at these wavelengths.

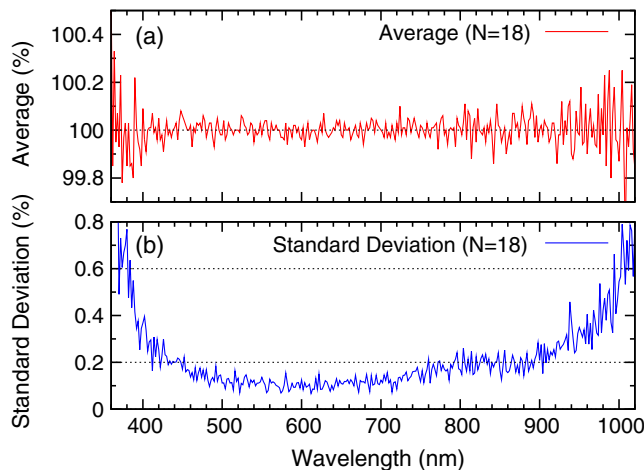


**Fig. 13** Statistical error evaluation of SPS. (a) and (b) The average and the standard deviation of 18 measurements of the optical path L, respectively, are shown.

## 8 Appendix B: Measurement Positions

The Subaru Telescope primary mirror of 8.3 m in diameter is mounted on the telescope, and it has limited accessibility. To carry out the *in-situ* measurement, we normally open the side covers of the telescope and then access the primary mirror from its side. Although the side covers open, there are telescope structures around the primary mirror and those structures restrict accessing to the primary mirror. This is the cause of the restricted measuring positions at the edge. For the center part, we have no way to access at all. Thus, we have monitored the reflectivity only at a few particular positions. The positions of the reflectivity measurements are shown in Fig. 14.

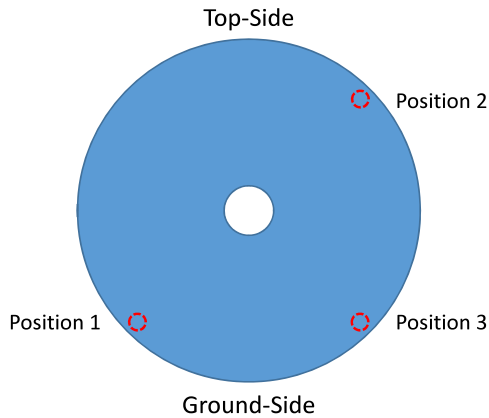


**Fig. 14** Locations on the Subaru Telescope primary mirror, where we monitor its reflectivity using SPS.

### Acknowledgments

This study is conducted as a part of the Subaru Telescope 8<sup>th</sup> primary mirror recoating project. We acknowledge all the project members, who carried out the 8<sup>th</sup> recoating work safely and completed successfully, especially Telescope Engineering Division members. Mr. H. Iwashita, Mr. H. Tsutsui, Mr. S. Nagayama, and Ms. R. Murai helped to measure the reflectivity. H.O. wishes to thank Dr. Y. Minowa and Dr. E. Mieda for much advice. Thanks Brian, too. We would also like to acknowledge the Subaru Telescope community and users, who pointed out the reflectivity degradation and encouraged us to develop SPS. This paper has been revised and updated from the SPIE conference proceedings.<sup>13</sup> Finally, the authors wish to recognize and acknowledge the very significant cultural role and reverence that the summit of Maunakea has always had within the indigenous Hawaiian community. We are most fortunate to have the opportunity to conduct observations from this mountain.

### References

1. K. Balasubramanian et al., "Aluminum mirror coatings for UVOIR telescope optics including the far UV," *Proc. SPIE* **9602**, 96020I (2015).
2. A. Feller et al., "Reflectivity, polarization properties, and durability of metallic mirror coatings for the European Solar Telescope," *Proc. SPIE* **8450**, 84503U (2012).
3. P. Dunlop et al., "Ethylene glycol contamination effects on first surface aluminized mirrors," *Proc. SPIE* **9906**, 99063F (2016).
4. B. Magrath, "Reflectivity degradation rates of Aluminum coatings at the CFHT," *Publ. Astron. Soc. Pac.* **109**, 303–306 (1997).
5. P. Giordano and M. S. Sarazin, "Survey of airborne particle density and the aging of mirror coatings in the open air at the VLT Observatory," *Proc. SPIE* **2199**, 977–985 (1994).
6. M. Abril-Abril et al., "Mirror coating and cleaning methodology to maintain the optical performance of the GTC telescope," *Proc. SPIE* **9906**, 99063U (2016).
7. T. Usuda et al., "Subaru Telescope: current performances and future upgrade plans," *Proc. SPIE* **5489**, 278–287 (2004).
8. P. Giordano and A. Torrejon, "In-situ cleaning of the NTT main mirror by CO<sub>2</sub> snow-flake sweeping," *Messenger* **75**, 9–11 (1994).
9. T. Noguchi et al., "Coating and cleaning of the Subaru Telescope mirrors," *Proc. SPIE* **4003**, 391–395 (2000).
10. J. W. Mayo and D. H. Killpatrick, "Scatter and reflectivity measurements on large telescope mirror coatings," *Prpc. SPIE* **3352**, 463–476 (1998).
11. M. Boccas et al., "Coating the 8-m Gemini telescopes with protected silver," *Proc. SPIE* **5494**, 239–253 (2004).
12. H. Okita, "Reflectivity of the Subaru Telescope's mirrors," Subaru Telescope, 2018 <https://www.naoj.org/Observing/Telescope/Parameters/Reflectivity/> (8 January 2019).
13. H. Okita, N. Takato, and S. S. Hayashi, "In-situ measurement of the Subaru Telescope primary mirror reflectivity," *Proc. SPIE* **10706**, 107061U (2018).

**Hirofumi Okita** is an assistant professor at Subaru Telescope, National Astronomical Observatory of Japan. He received his PhD degree from Tohoku University in 2014. His current research interests include air turbulence evaluation, monitoring of site environment, and degradation in optics.

Biographies of the other authors are not available.